High power generation of adaptive laser beams in a Nd:YVO₄ MOPA system

S. H. Noh, D. J. Kim, and J. W. Kim*

Department of Photonics and Nanoelectronics, Hanyang University ERICA, Ansan, 15588, South Korea
*Corresponding author: jwk7417@hanyang.ac.kr

We report efficient power scaling of the laser output with an adaptive beam profile from an Nd:YAG dual-cavity master oscillator using a three-stage end-pumped Nd:YVO₄ amplifier. We succeed in the fast switching of an excited laser mode by modulating an acousto-optic modulator loss in a dual-cavity master oscillator, thereby achieving temporal modulation of the output beam profile. The outputs from the master oscillator are amplified via a three-stage power amplifier yielding 36.6, 40.5, and 45.4 W of the maximum output at 116.8 W of incident pump power for the transverse electromagnetic, Laguerre–Gaussian, and quasi-top-hat beam, respectively. The prospects for further power scaling and applications via the dual-cavity master-oscillator power-amplifier (MOPA) system are considered.

OCIS codes: 080.4865, 140.0140, 140.3280, 140.3300, 140.3410, 140.3530.
doi: 10.3788/COL201715.120801.

Diode-end-pumped solid state lasers are used in numerous applications in areas such as industry, defense, medicine, and spectroscopy, due to their low lasing thresholds, high optical efficiencies, and simple configuration[1]. One of the main attractions in this laser architecture is to selectively excite one or a few transverse modes in the laser resonator simply by shaping the pump light distribution in the gain medium, resulting in generation of a laser beam with desirable intensity distribution, for example, Gaussian, top-hat, and donut-shaped profiles. However, it is difficult to switch the excited laser mode in the fixed resonator configuration without loss of power or efficiency, since it is generally optimized for the targeted mode. The simplest way to select and switch the resonator mode is to insert an aperture (AP) in the resonator[1]. This method is widely used, but works only for suppressing higher-order modes. Mode selection can be also achieved using programmable spatial phase plates in the cavity (e.g., liquid crystal spatial light modulators[2,3] or computer generated holograms[4,5]). However, scaling to high powers via this route is challenging due to their power handling limitations and high losses. A dual-pumping configuration, i.e., using two independent pump beams with quasi-Gaussian and donut-shaped intensity distributions, has been shown to be effective in selecting and switching the excited laser mode, but this does require a complex pumping system, such as a capillary fiber[6,7].

Recently, we reported the simple alternative strategy for selecting an excited mode in an end-pumped solid state laser employing a coupled dual-cavity configuration[8–10]. In this configuration, we can not only select the excited mode in the laser resonator but also control the relative contributions of the two different modes in the primary cavity by a simple adjustment of the round-trip loss in the independent secondary cavity. We have successfully applied this scheme to the diode-pumped Nd:YAG laser

for the selective generation of a fundamental transverse electromagnetic (TEM₀₀) or Laguerre–Gaussian (LG₀ₙ, $n = 1, 2, 3$) mode with high efficiency. Moreover, we were able to successfully produce a laser beam with tailored intensity distribution by adjusting the ratio of the respective contributions of the TEM₀₀ mode to the LG₀₁ mode in the output beam. However, the maximum output power was limited to a few watts due to the induced thermal lensing and energy migration in the gain medium.

In this Letter, we report a high power, high efficiency Nd:YVO₄ master-oscillator power-amplifier (MOPA) system with adjustable beam profiles incorporating an Nd:YAG dual-cavity master oscillator and three Nd:YVO₄ end-pumped amplifier stages. The MOPA can produce the maximum output powers of 36.6, 40.5, and 45.4 W with extraction efficiencies for the three-stage amplifier of 31.2%, 34.6%, and 38.8% for the TEM₀₀, LG₀₁, and quasi-top-hat mode beams, respectively. Moreover, we report fast switching of the excited mode in the resonator and, as a result, dynamic modulation of the output beam profile simply by modulating the acousto-optic modulator (AOM) loss in the dual-cavity master oscillator.

The dual-cavity master oscillator setup used in our experiment is shown in Fig. 1. The laser employs a coupled
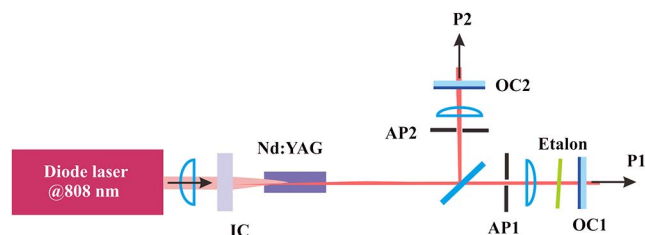

Fig. 1. Experimental setup for an Nd:YAG dual-cavity master oscillator.

dual-cavity configuration, i.e., the primary and secondary cavities share a common gain medium and pump-in-coupling mirror, then separate through a thin-film polarizer to two linear cavities with the perpendicularly polarized cavity modes, as described in more detail in Ref. [8]. In this setup, a 1.0 at.% Nd:YAG with 5 mm in length was used as the gain medium and mounted in a water-cooled aluminum heat sink maintained at 19°C positioned in close proximity to the pump-in-coupling mirror. The pump beam was provided by a fiber-coupled diode laser at 808 nm. The pump absorption efficiency in the Nd:YAG rod was measured to be ∼80% under optimum operating conditions.

The primary cavity comprised a plane pump input coupler (IC) with high reflectivity (>99.8%) at the lasing wavelength (∼1 μm) and high transmission (>95%) at the pump wavelength (808 nm), a plano-convex lens of 75 mm focal length antireflection (AR)-coated at the lasing wavelength, and a plane output coupler with 20% transmission at the lasing wavelength (OC1). In order to excite both the TEM_{00} and LG_{01} modes simultaneously, the pump beam was focused to have a waist radius of ∼220 μm in the crystal, since the calculated TEM_{00} waist was ∼170 μm[7].

The secondary cavity included the shared pump IC, a second AR-coated lens of a 75 mm focal length, and a plane output coupler with 5% transmission at the lasing wavelength (OC2). The secondary cavity also had a similar TEM_{00} mode size in the gain medium compared to the primary cavity. An AP was inserted to suppress higher-order modes in the secondary cavity, especially the LG_{01} mode in this experiment. Furthermore, we placed an AOM in the secondary cavity to provide a tunable cavity loss for the TEM_{00} mode, still resulting in a lower lasing threshold than for the primary cavity. Under this configuration, we were able to define the spatial gain distribution in the gain medium, resulting in the generation of the laser output beam with a spatial intensity distribution ranging from a pure donut beam to one with a quasi-top-hat profile, simply by controlling the AOM diffraction loss[9]. Figure 2 shows the laser output powers as a function of absorbed pump power for the TEM_{00}, LG_{01}, and quasi-top-hat mode beams. The insets are the measured beam profiles with the aid of the silicon CCD beam profiler. The laser yielded 2.8, 3.1, and 4.0 W of the maximum outputs at 11.6 W of absorbed pump power, corresponding to the slope efficiencies of 34.8%, 38.2%, and 47.6%, for the TEM_{00}, LG_{01}, and quasi-top-hat beams, respectively. The beam qualities at the maximum powers were measured to be 1.01, 1.98, and 1.70 for the TEM_{00}, LG_{01}, and quasi-top-hat beams, respectively, confirming that the excited modes were the targeted modes. Moreover, we modulated the AOM diffraction loss with repetition rates of 1 and 100 Hz. When the AOM was off, the output from the primary cavity (P1) was the LG_{01} mode beam, but, when it was on, the output beam had the quasi-top-hat intensity profile due to simultaneous excitation of the
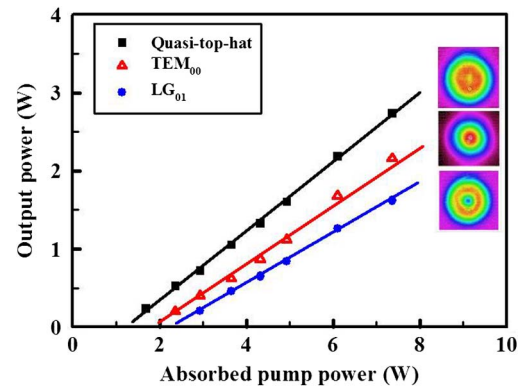

Fig. 2. (Color online) Output power (P1) of the TEM_{00}, LG_{01}, and quasi-top-hat beams from the Nd:YAG dual-cavity master oscillator as a function of incident pump power.

TEM_{00} and LG_{01} modes. In order to see the modulation speed of the beam profile, we measured the output power through a pinhole placed at the center and edge of the beam with the aid of a fast photo-detector. The results clearly show in Fig. 3 that the excited laser mode was quickly switched, resulting in fast modulation of the output beam profile. The slight increase of the power at the edge for the quasi-top-hat-shaped beam was due to contributions from the wing of the excited TEM_{00} mode to the existing LG_{01} mode. Therefore, it is highlighted that this dual-cavity allows us to achieve selective excitation and fast switching of the laser resonating mode and, as a result, dynamic modulation of the output beam profile in the simple way. The laser outputs from this dual-cavity master oscillator were amplified in the following amplifier stage. The incident power to the first amplifier was fixed at 0.5 W regardless of the beam profile.

The output from the dual-cavity master oscillator was launched to a three-stage end-pumped $Nd:YVO_4$ amplifier, as shown in Fig. 4. The first and second amplifier stages comprised a 10 mm long $Nd:YVO_4$ crystal mounted in water-cooled aluminum heat sinks maintained at 19°C. The crystal had a low Nd concentration of 0.1 at.% to reduce the generated heat and detrimental thermal effects due to the energy transfer upconversion[11,12]. Each $Nd:YVO_4$ crystal was end-pumped by a high power diode laser at 808 nm coupled to a single-clad multimode fiber with a 105 μm core diameter. The signal light enters and exits the amplifier modules with the aid of two dichroic mirrors orientated at 45° with high reflectivity (>99.8%) at 1064 nm and high transmission (>95%) at 808 nm. This end-pumped amplifier configuration is attractive, since it offers the prospect of high efficiency due to the good overlap between the pump and signal beams. However, phase aberration of the thermal lensing in the gain medium, due to the high pump deposition density and its non-uniform transverse intensity profile, may lead to significant degradation in beam quality[13], which is given by
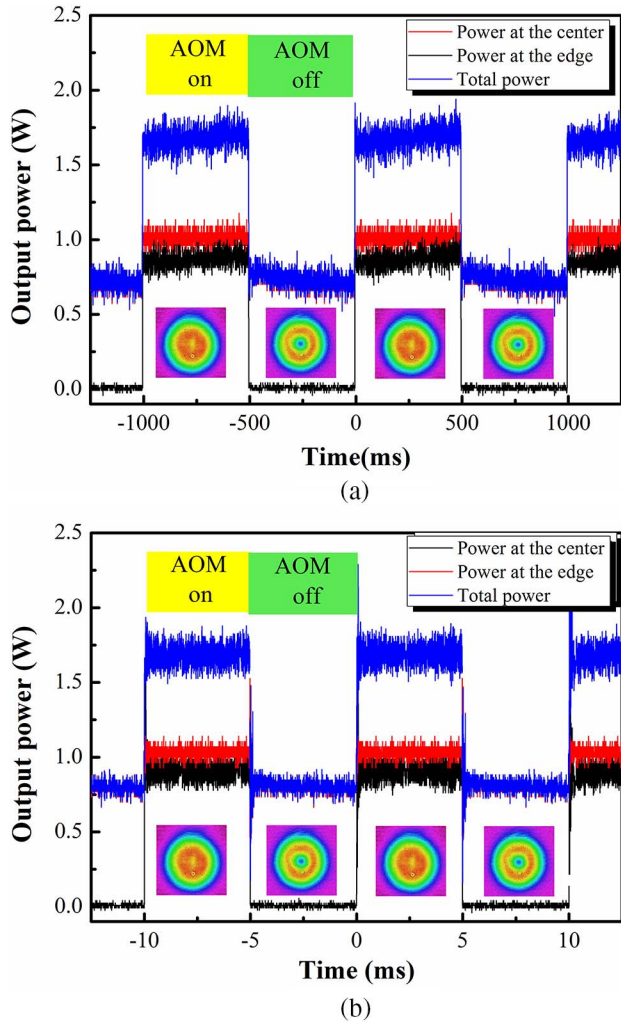
Fig. 3. (Color online) Temporal modulation of the output beam profiles due to the AOM on/off. The power was measured at the center and the edge of the beam at repetition rates of (a) 1 and (b) 100 Hz. The insets are the measured transverse intensity distribution by the CCD camera.

$$M_f^2 = \sqrt{(M_i^2)^2 + (M_q^2)^2}. \tag{1}$$

Here, M_i^2 is the initial beam quality factor, and M_q^2 is the quartic phase aberration due to the thermal lensing aberration. Assuming that the pump beam has a Gaussian intensity distribution and the signal beam is smaller than the pump beam, the latter factor is expressed as

$$M_q^2 = \frac{2P_{\mathrm{abs}}(\mathrm{d}n/\mathrm{d}T)}{K_c \lambda \sqrt{2}} \left(\frac{w_L}{w_p}\right)^4, \tag{2}$$

where P_{abs} is the absorbed pump power, $\mathrm{d}n/\mathrm{d}T$ is the change of refractive index with temperature, K_c is the thermal conductivity, λ is the wavelength, and w_L/w_p is the laser/pump beam radius. Equation (2) indicates that a smaller signal beam is better for achieving a good beam quality in the amplifier. However, a lower extraction efficiency is inevitable for the smaller signal beam[14–17].
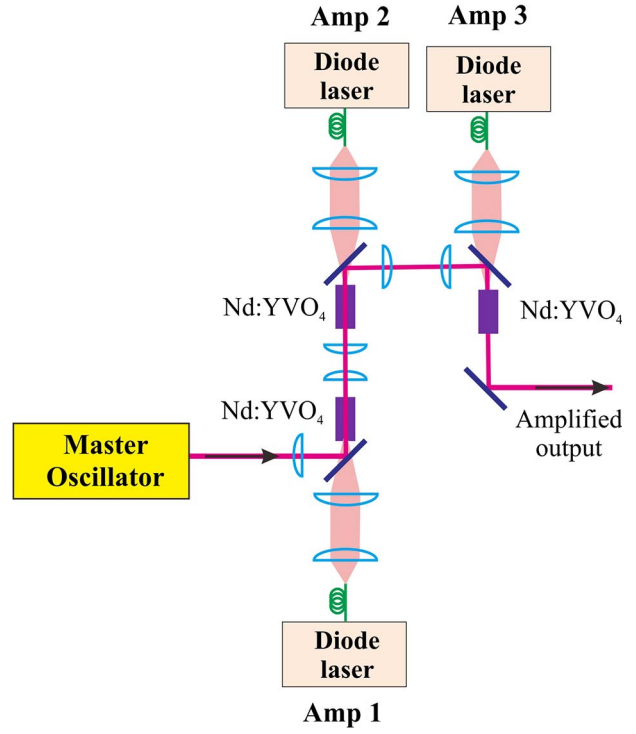

Fig. 4. Schematic diagram of the master oscillator and the three-stage Nd:YVO$_4$ power amplifier system.

Therefore, we should maximize the brightness B of the amplified output beam defined by

$$B = \frac{CP}{\lambda^2 M_x^2 M_y^2}, \tag{3}$$

where P is the power, and C is the constant that depends on the beam profile (for a Gaussian beam profile, $C = 1$)[1]. Thus, careful optimization of the signal and pump beam sizes is required by monitoring the output power and the beam quality. In this experiment, we matched the signal beam size of the quasi-top-hat intensity distribution to the pump beam, which had a focused beam size of ~350 and ~500 μm in the first and second Nd:YVO$_4$ crystals, respectively. Two plano-convex lenses with focal lengths of 50 and 75 mm were placed between the crystals for relay imaging. The unabsorbed pump light after the first pass of each crystal was also relay imaged to the other crystal, leading to an increase of the overall pump absorption efficiency. For amplification of the different modes, i.e., the TEM$_{00}$ or LG$_{01}$ modes, we simply adjusted the diffraction loss of the AOM for exciting the targeted mode in the master oscillator under the same arrangement. The focused beam size of the TEM$_{00}$ mode was ~68% of the quasi-top-hat beam, and the outer diameter of the LG$_{01}$ mode was nearly the same as that of the quasi-top-hat beam[8]. The third amplifier stage also used a 0.1 at.% Nd:YVO$_4$ crystal with 15 mm in length. The pump and quasi-top-hat signal beams were focused to a beam diameter of ~750 μm in the crystal. The size of the pump and

the signal beams were increased in the following amplifiers to reduce the heat deposition density and beam quality degradation due to the induced thermal lensing aberration. The pump powers delivered to the $Nd:YVO_4$ crystals were 35, 60, and 60 W, respectively.

The output power from the three-stage amplifier as a function of incident pump power is shown in Fig. 5. The maximum continuous-wave (CW) output powers achieved were 36.6, 40.5, and 45.4 W at a combined pump power of 116.8 W, corresponding to the extraction efficiencies of 30.9%, 34.2%, and 38.5% for the TEM_{00}, LG_{01}, and quasi-top-hat beams, respectively. Figure 6 shows the near-field beam profiles and the measured M^2 parameters of the output beams after the first, second, and third amplifier stages at the maximum pump powers. The beam qualities at the maximum pump powers were measured to be 1.13, 2.01, and 1.91 for the TEM_{00}, LG_{01}, and quasi-top-hat beams, respectively, which were slightly increased from those of the master oscillator. These results confirm that the seed beam characteristics, including the beam intensity distribution, were well maintained in the MOPA arrangement. However, it is noticed that the intensity in the center of the LG_{01} mode beam did not become zero, which was ~10% of the peak value. We believe that this was amplified spontaneous emission due to the pump beam with quasi-Gaussian intensity distribution in the amplifiers. Moreover, the dynamic modulation of the amplified output beam was also achieved when we modulated the output beam profile of the dual-cavity master oscillator, as seen in Fig. 3. Therefore, it would be possible to realize fast switching of the output mode and dynamic modulation of the output beam profile in power levels of multi-hundred watts by employing a higher pump power source or an additional amplifier. Furthermore, generation of the high peak power laser pulses with a tailored transverse intensity profile via Q-switching or mode-locking would be very useful in many applications, which is an on-going work.

(a)

(b)

(c)

Fig. 6. (Color online) (a) Output beam profiles, (b) theoretical and measured transverse intensity distributions for top-hat, TEM_{00}, and LG_{01} mode beams, and (c) the measured beam qualities after the master oscillator and each amplifier stage at the maximum output power.
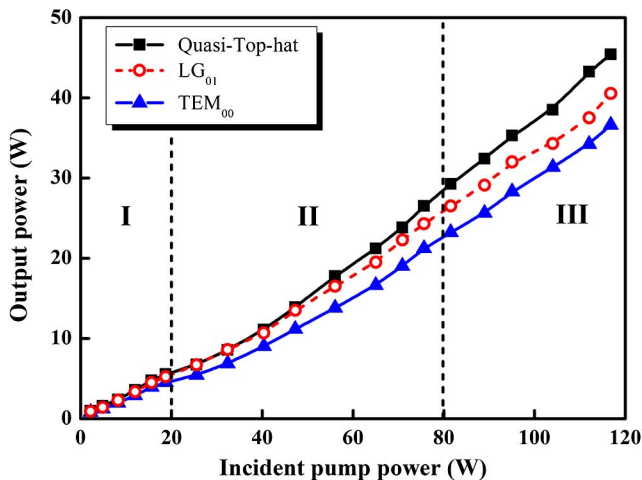

Fig. 5. (Color online) Output power from the three-stage amplifier as a function of incident pump power. The signal input power was fixed to 0.5 W regardless of the beam profile.
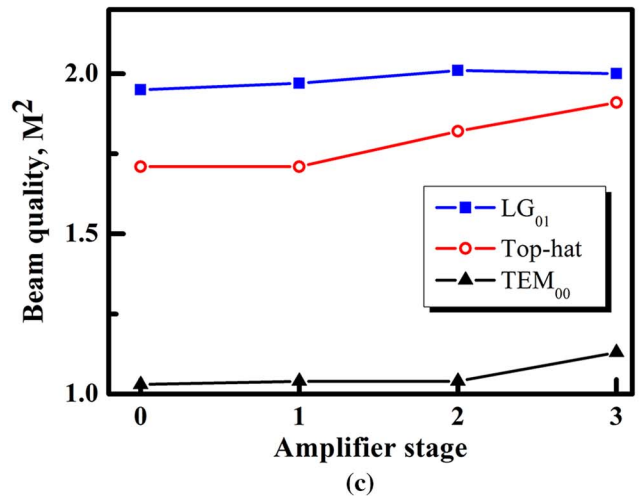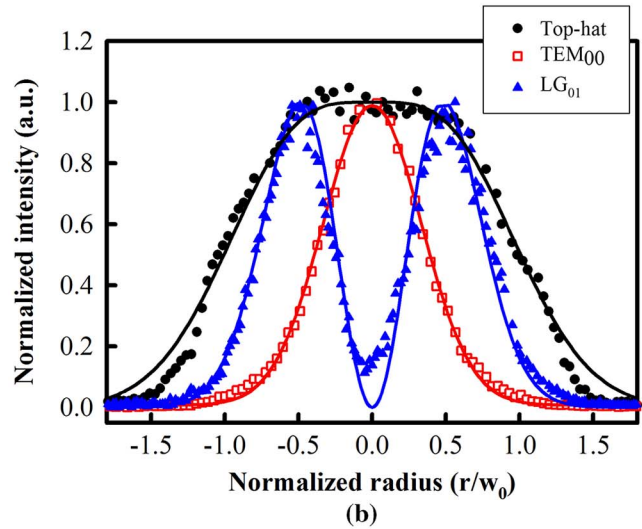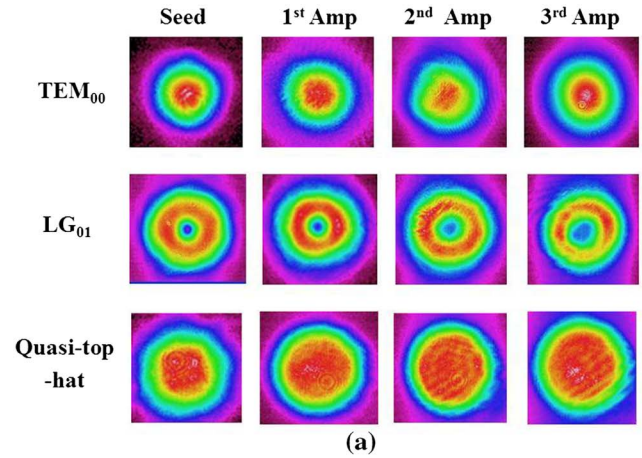
In conclusion, we demonstrate efficient power scaling and the fast mode switching of the laser output from an Nd:YAG master oscillator using a three-stage end-pumped $Nd:YVO_4$ amplifier. The MOPA yields 36.6, 40.5, and 45.4 W of the maximum output at 116.8 W

of incident pump power for TEM_{00}, LG_{01}, and quasi-top-hat beams, respectively. Degradation in the beam quality due to the thermal effects is minimized by employing an optimized amplifier design, including the signal–pump overlap and $Nd:YVO_4$ with a low Nd doping concentration. This design proves that the output beam profile tailored in the master oscillator is well maintained in the amplifiers, resulting in amplified output beams with $M^2 \approx 1.13$, 2.01, and 1.91 for the TEM_{00}, LG_{01}, and quasi-top-hat beams, respectively. Furthermore, we successfully achieve fast modulation of the output beam profile simply by controlling the AOM diffraction loss of the secondary cavity in the dual-cavity master oscillator. This approach is advantageous for high power solid state laser systems requiring adaptive beam profiles, temporal modulation of the spatial intensity distribution, and good extraction efficiency of the stored energy. Therefore, we believe that the simplicity and flexibility afforded by this technique will benefit a range of applications requiring laser beams with high power and a bespoke intensity profile.

References

1. W. Koechner, *Solid State Laser Engineering* (Springer-Verlag, 2006), p. 407.
2. V. Bagnoud and J. D. Zuegel, Opt. Lett. **29**, 295 (2004).
3. X. Wang, J. Ding, W. Ni, C. Guo, and H. Wang, Opt. Lett. **32**, 3549 (2007).
4. N. R. Heckenberg, R. McDuff, C. P. Smith, and A. G. White, Opt. Lett. **17**, 221 (1992).
5. J. Arlt, K. Dholakia, L. Allen, and M. J. Padgett, J. Mod. Opt. **45**, 1231 (1998).
6. J. W. Kim, J. I. Mackenzie, J. R. Hayes, and W. A. Clarkson, Opt. Lett. **37**, 1463 (2012).
7. J. W. Kim and W. A. Clarkson, Opt. Commun. **296**, 109 (2013).
8. D. J. Kim and J. W. Kim, Appl. Phys. B **121**, 401 (2015).
9. D. J. Kim, J. I. Mackenzie, and J. W. Kim, Opt. Lett. **41**, 1740 (2016).
10. D. J. Kim and J. W. Kim, Opt. Commun. **383**, 26 (2017).
11. P. J. Hardman, W. A. Clarkson, G. J. Friel, M. Pollnau, and D. C. Hanna, IEEE. J. Quantum Electron. **35**, 647 (2002).
12. J. W. Kim, J. I. Mackenzie, and W. A. Clarkson, Opt. Express **17**, 11935 (2009).
13. W. A. Clarkson, J. Phys. D Appl. Phys. **34**, 2381 (2001).
14. B. J. Neubert and B. Eppich, Opt. Commun. **250**, 241 (2005).
15. J. W. Kim, M. J. Yarrow, and W. A. Clarkson, Appl. Phys. B **85**, 539 (2006).
16. S. Kanazawa, Y. Kozawa, and S. Sato, Opt. Lett. **39**, 2857 (2014).
17. Y. Li, W. Li, Z. Zhang, K. Miller, R. Shori, and E. G. Johnson, Opt. Express **24**, 1658 (2016).